Dynamic reliability of nonlinear systems under random excitation

Fritz Colonius, G. Häckl, Wolfgang Kliemann

Angaben zur Veröffentlichung / Publication details:

Colonius, Fritz, G. Häckl, and Wolfgang Kliemann. 1995. "Dynamic reliability of nonlinear systems under random excitation." In *Proceedings of the 1995 Design Engineering Technical Conferences: presented at the 1995 ASME Design Engineering Technical Conferences, Boston, MA, USA, September 17–21, 1995; Volume 3, Part A: Vibration of nonlinear, random, and time-varying systems*, edited by S. C. Sinha, B. F. Spencer, J. P. Cusumano, Aldo A. Ferri, Friedrich Pfeiffer, M. Akif Özbek, A. K. Bajaj, et al., 1007–24. New York, NY: American Society of Mechanical Engineers.

DE-Vol. 84-1

Proceedings of the
1995 DESIGN ENGINEERING
TECHNICAL CONFERENCES

VOLUME 3
PART A

VIBRATION OF NONLINEAR, RANDOM, AND TIME-VARYING SYSTEMS

presented at

THE 1995 ASME DESIGN ENGINEERING TECHNICAL CONFERENCES –
THE 15TH BIENNIAL CONFERENCE ON MECHANICAL VIBRATION AND NOISE
SEPTEMBER 17–20, 1995
BOSTON, MASSACHUSETTS

sponsored by

THE DESIGN ENGINEERING DIVISION, ASME

compiled by

H. H. CUDNEY
VIRGINIA POLYTECHNIC INSTITUTE

edited by

S. C. SINHA
AUBURN UNIVERSITY

B. F. SPENCER, JR.

J. P. CUSUMANO

ALDO A. FERRI
GEORGIA TECH

FRIEDRICH PFEIFFER
TECHNISCH UNIVERSITAT MUNCHEN

M. AKIF ÖZBEK
THE BOEING COMPANY

A. K. BAJAJ

A. SOOM
UNIVERSITY OF BUFFALO

RAOUF A. IBRAHIM
WAYNE STATE UNIVERSITY

D. E. NEWLAND
CAMBRIDGE UNIVERSITY

L. A. BERGMAN
UNIVERSITY OF ILLINOIS–URBANA CHAMPAIGN

THE AMERICAN SOCIETY OF MECHANICAL ENGINEERS
UNITED ENGINEERING CENTER / 345 EAST 47TH STREET / NEW YORK, N.Y. 10017

DE-Vol. 84-1, 1995 Design Engineering Technical Conferences
Volume 3 — Part A
ASME 1995

DYNAMIC RELIABILITY OF NONLINEAR SYSTEMS UNDER RANDOM EXCITATION

Fritz Colonius
Institut für Mathematik
Universität Augsburg
Augsburg, Germany

Gerhard Häckl
Department of Mathematics
Iowa State University
Ames, IA
and
Institut für Mathematik
Universität Augsburg
Augsburg, Germany

Wolfgang Kliemann
Department of Mathematics
Iowa State University
Ames, IA

ABSTRACT

Reliability theory analyzes failure phenomena in systems, leading to maintenance and replacement schedules as well as risk assessment and other topics. Dynamic reliability takes into account the (possibly nonlinear) dynamics of the system and of the random excitation that may lead to failure. It is shown, how some of the concepts of reliability theory can be interpreted in the dynamical systems context. Analytical results are derived for failure probabilities, for life time distributions, asymptotic damage accumulation rates, and other relevant concepts. The Takens-Bogdanov oscillator and a model for ship roll motion are analyzed in detail, together with a thorough description of the numerical methods that are available for dynamic reliability studies.

1. INTRODUCTION

In reliability theory one usually distinguishes between two scenarios that can lead to failure : Collapse (abrupt failure) and fatigue (often called aging), accumulated under various operating conditions over time. The first phenomenon is often indicated by a binary variable Y switching from 0 (operating to 1 (failed) at some random time T. The statistical description of this scenario relies on the life time distribution of Y, i.e. on the distribution $P\{T > t\} = P\{Y(t) = 0\}$, and on the failure probability $P\{Y(t) = 1\}$ at time t. If the random variable Y is observable, a variety of statistical estimation and prediction methods are available that apply to various sampling schemes and error models. An important modification of this approach also records the failed component, i.e. Y is a random variable taking on finitely many values $0 \dots n$, where $Y(T) = i$, $i = 1 \dots n$ indicates that component i has failed. In this case the fault distribution $P\{Y(T) = i\}$ allows the identification of weak components in a system. In the second case the failure variable Y is often taken to be continuous, i.e. real valued, and $Y(t)$ increases until a certain threshold Λ, indicating fatigue failure, is reached. The statistical description of this scenario again relies on the life time distribution $P\{T > t\} = P\{Y(t) < \Lambda\}$ and on the

Partially supported by DFG grant no. Co 124/12-1 and by ONR grant no. N00014-93-1-0868

failure probability $P\{Y(t) \geq \Lambda\}$ at time t. Estimation and prediction methods for this case can be found e.g. in Barlow and Proschan (1975) or Mann et al. (1974). In both scenarios the statistical analysis leads to maintenance and replacement schedules as well as risk assessment and other practical studies.

Dynamic reliability adds a dynamical systems aspect to the picture described above. The system itself is now modeled by a set of differential equations, describing its behavior in time. Random perturbations, modeled by stochastic processes, act on the system and drive it out of its operating point. These perturbations can be external (environmental, random forcing), leading to additive terms in the system equations, or internal (parameter excitation), leading to multiplicative terms, i.e. stochastic terms with their own dynamics. These systems may be modeled as random differential equations of the form

$$\dot{x} = X_0(x) + \sum_{i=1}^{m} \xi_i(t) X_i(x) \tag{1}$$

where x is a state space description of the system, $\dot{x} = X_0(x)$ is the undisturbed system dynamics, $\xi_i(t)$, $i = 1 \ldots m$ are the random perturbations and X_i are the perturbation dynamics, with $X_i(x) \equiv 1$ if the perturbation ξ_i is external. Note that e.g. in many physical and chemical systems the form and the parameters of the vector fields $X_0 \ldots X_m$ are obtained from scientific principles. Furthermore, many characteristics of the random processes $\xi_1 \ldots \xi_m$ are available through measurements of the perturbation alone, such as perturbation range, spectrum, correlation times etc.

The two common reliability scenarios as described above, can now be interpreted in the dynamical context of the system (1). Collapse corresponds to crossing of a threshold set L by the system response $\psi(t, x_0, \omega)$, where ψ denotes the solution of (1) with initial value x_0. The life time T is the first exit time of the system from L, i.e. $T = \tau_L(x_0) = \inf\{t \geq 0,\ \psi(t, x_0, \omega) \in L^c\}$. ($L^c$ is the complement of the set L.) Failure probabilities (at time t) are then defined in the obvious way, and the fault distribution is the random variable $H(x_0) = \{x, x = \psi(T, x_0, \omega)\}$. The statistics of these random variables contain the information for maintenance and replacement schedules, and for risk assessment of random dynamical systems.

The second scenario, failure due to fatigue accumulation, can be modeled in two different ways for randomly perturbed dynamical systems. One is the dynamical description of fatigue phenomena themselves, e.g. in the form of crack propagation. We refer the reader to the survey (Bolotin, 1995) for details on this approach. The other possibility is adapting the statistical concept mentioned above: If the damage experienced by a system at time t depends on the state of the system at time t, the one can measure the accumulated damage up to time t as $F(t, x_0, \omega) = \int_0^t f(\psi(s, x_0, \omega))ds$, where f is a damage function defined on the state space of the system. The life time T is then the random variable describing the first time the process $F(t, x_0, \omega)$ reaches a certain threshold Λ, and for $t \geq 0$ fixed, $F(t, x_0, \cdot)$ is the random damage level at time t, in particular $P\{F(t, x_0, \omega) \geq \Lambda\}$ is the failure probability at time t. Again, these random variables contain all the information for maintenance and replacement scheduling, as well as for risk assessment based on damage accumulation in randomly excited dynamical systems.

In this paper we study random dynamical systems with respect to collapse and damage accumulation as described above. The system model is Equation (1), and we assume that the random perturbation $\xi(t)$ is a functional of a bounded, stationary diffusion process. In particular, we consider a family $\{U_\rho \subset \mathbb{R}^m, \rho \geq 0\}$ of perturbation ranges, i.e. sets in which $\xi(t)$ takes its values, and we analyze the effect of varying perturbation ranges on the reliability behavior of the system. Thus the random excitation in our set-up is neither a Gaussian process, nor do we assume that the excitation is small.

The undisturbed system $\dot{x} = X_0(x)$ itself can have a rather complex behavior: Besides equilibrium points and periodic orbits, homoclinic orbits and, in higher dimensions, chaotic behavior can occur. Non-Gaussian random perturbations, together with possibly nonlinear excitation dynamics, further complicate the study of the system (1). Some analytical techniques, based on the so-called support theorem (Stroock and Varadhan, 1972), are available to study the long term qualitative behavior of these systems. However, the reliability concepts are finite time concepts. We will present various analytical results that address some aspects of these concepts. Our approach uses the classical theory of Markov diffusion processes. For small perturbations of two dimensional systems with homoclinic orbit, an approach to exit time computations around the homoclinic orbit has recently been proposed, see Frey and Simiu (1993). The idea is based on a small noise version of Melnikov functions and results in asymptotic expansions of exit statistics. Using Markov diffusion theory for systems as general as (1) in dimension ≥ 2, one cannot obtain explicit analytical expressions for the statistics of the random variables important in reliability theory. Instead, one has to use efficient nu-

merical techniques for the analysis of specific systems. These techniques, as presented below, are a combination of global orbit computations for perturbed dynamical systems and of numerical solutions for stochastic differential equations.

In Section 2. we present some analytical results on collapse and damage accumulation for randomly excited dynamical systems. After a brief review of the qualitative behavior of stochastic systems of the type (1), we characterize the failure probabilities, the fault distribution, and the expectation of the life time distribution for the collapse scenario. Considering the damage accumulation scenario, we study the expectation of the life time distribution and compute the asymptotic damage accumulation rate. Section 3. contains the detailed analysis of the Takens-Bogdanov oscillator with respect to collapse and damage accumulation phenomena. In this section our approach to numerical methods for dynamic reliability problems is also thoroughly explained. We have chosen the Takens-Bogdanov oscillator for this study because it presents various of the complexities of two dimensional systems, including periodic and homoclinic orbits, stationary and transient solutions, as well as bistability behavior. Finally, Section 4. is devoted to a model of ship roll motion (Thompson et al., 1993). Here we study the various aspects of collapse, i.e. of capsizing in a random sea.

2. COLLAPSE AND DAMAGE ACCUMULATION – ANALYTICAL RESULTS

2.1. THE MATHEMATICAL MODEL

In this paper we consider nonlinear dynamical systems given by ordinary differential equations on a finite dimensional state space, i.e.

$$\dot{x} = X_0(x), x \in M. \tag{1}$$

Here X_0 is a C^∞ vector field on a d-dimensional ($1 \leq d < \infty$) C^∞ manifold M. The system (1) operates at a stable limit set, e.g. a fixed point, a periodic motion, or a stable chaotic attractor. In this operating mode, the system is disturbed by a random parametric or additive excitation, resulting in the model

$$\dot{x} = X_0(x) + \sum_{i=1}^{m} \xi_i(t) X_i(x) \text{ on } M, \tag{2}$$

where $\xi(t) = (\xi_i(t),\ i = 1 \ldots m)$ is a stochastic process, and $X_i(x)$, $i = 1 \ldots m$, are the (smooth) excitation dynamics. We model the excitation $\xi(t)$ as a functional of an underlying stationary, ergodic diffusion process of the form

$$d\eta(t) = Y_0(\eta(t))dt + \sum_{j=1}^{\ell} Y_j(\eta(t)) \circ dW_j \text{ on } N, \tag{3}$$

where N is a C^∞ manifold (of finite dimension), $Y_0 \ldots Y_\ell$ are C^∞ vector fields on N, "$\circ$" denotes the symmetric (Stratonovič) stochastic differential. We assume throughout this paper:

- $\eta(t)$ is stationary and ergodic hence admits on invariant distribution λ on N with C^∞ density.
- Equation (3) is nondegenerate in the sense that the Lie algebra $\mathcal{LA}(Y_1, \ldots, Y_\ell)$ generated by the diffusion vector fields $Y_1 \ldots Y_\ell$ has full rank at each point $p \in N$, i.e. $\dim \mathcal{LA}(Y_1, \ldots, Y_\ell)(p) = \dim N$. This condition is weaker than the standard ellipticity condition for stochastic differential equations, see e.g. Kliemann (1988) for a discussion of nondegeneracy.
- The noise space N is compact, ruling out excitation processes with Gaussian statistics, and leading to more realistic models of macroscopic (non atomic) systems.

In order to study the behavior of the randomly excited system (2) depending on the strength of the excitation, we consider an increasing family $\{U_\rho, \rho \geq 0\}$ in $\mathbb{R}^m$ of compact excitation ranges, and a family $\{f_\rho, \rho \geq 0\}$ of C^∞ onto maps

$$f_\rho : N \to U_\rho,\ f_\rho(\eta(t)) = \xi(t) \tag{4}$$

mapping the background noise $\eta(t)$ onto the random excitation $\xi(t)$ in U_ρ. Note that $\xi(t)$ is a stationary process, but not necessarily Markovian. The pair process $(\eta(t),\ x(t))$ is, however, a Markov diffusion process for all $\rho \geq 0$, compare e.g. Kliemann (1987). A typical family of excitation ranges is of the form $U_\rho = \rho \cdot U$, where $U \subset \mathbb{R}^m$ is compact with 0 in its interior. For $\rho = 0$ we obtain the undisturbed system (1), and with increasing ρ the system is subject to large and larger excitations.

The set-up described above allows us to study dynamic reliability aspects of the system (2) depending on the parameter ρ. We will analyze collapse and damage accumulation effects as they vary with the excitation range ρ.

Frequently, it is also of interest to analyze the behavior with respect to an additional bifurcation parameter $\alpha \in \mathbb{R}^p$ ($1 \leq p < \infty$). This results in the model

$$\dot{x} = X_0(x, \alpha) + \sum_{i=1}^{m} \xi_i(t) X_i(x, \alpha) \text{ on } M \tag{5}$$

with excitation ξ as above. For fixed ρ we can identify the optimal α for which failure probabilities are smallest, or failure times are largest. This aspect applies e.g. to systems in which α represents a tuning parameter (e.g. material constant) that can take different values depending on specific designs.

2.2. QUALITATIVE BEHAVIOR OF STOCHASTIC SYSTEMS

The mathematical model described in Section 2.1. is rather general: The system dynamics, the excitation dynamics, and the underlying noise process are all nonlinear, and the noise statistics are non-Gaussian. Hence one cannot expect to obtain explicit expressions for failure probabilities, failure distributions, etc. Even perturbation expansions are not available in this set-up. Some analytical results, however, can be obtained based on the qualitative theory of stochastic systems. We will present these results in Sections 2.3 and 2.4. To make the paper more self-contained, we review in this section some results that will be needed later on. For references see Kliemann (1987, 1988), Colonius and Kliemann (1994b), Colonius et al. (1995) and the references therein.

For the moment, fix the parameter ρ, the excitation range will be denoted by $U \subset \mathbb{R}^m$, convex, compact, with 0 in its interior. We associate to the randomly excited system (2) formally a control system

$$\dot{x} = X_0(x) + \sum_{i=1}^{m} u_i(t) X_i(x) \quad \text{on} \quad M, \tag{6}$$

where $U(t) = (u_i(t),\ i = 1 \dots m) \in \mathcal{U} = \{u : \mathbb{R} \to U$ measurable$\}$. We denote by $\varphi(t, x, u)$ the solution of (6) at time t, under the control $u \in \mathcal{U}$, and with fixed initial value $\varphi(0, x, u) = x$. Information about the random system (2) can be obtained by studying the control and limit structure of the system (6). For regular systems this mechanism is given by the support theorem (see e.g. Stroock and Varadhan (1972), Kunita (1974), or Ikeda and Watanabe (1981)), for singular systems the family of associated Lyapunov exponents plays a crucial role. In this paper, we restrict our attention to regular systems, i.e. we assume throughout

$$\text{(H)} \qquad \dim \mathcal{LA}(X_0 + \sum_{i=1}^{m} u_i X_i,\ u \in U)(x) = \dim M \quad \text{for all } x \in M.$$

Here $\mathcal{LA}(X_0 + \Sigma u_i X_i,\ u \in U)$ denotes the Lie algebra generated by the family of vector fields $\{X_0 + \Sigma u_i X_i,\ u \in U\}$.

The control and limit behavior of the system (6) is described by its control sets $C \subset M$ and their domains of attraction $\mathcal{A}(C)$ (Colonius and Kliemann, 1993, 1994a). Recall that a main control set C is a maximal subset of M with nonvoid interior such that $C \subset c\ell\mathcal{O}^+(x)$ for all $x \in C$, where $\mathcal{O}^+(x)$ is the positive orbit of x given by $\mathcal{O}^+(x) = \{y \in M,$ there exist a piecewise constant $u \in \mathcal{U}$ and $t \geq 0$ with $\varphi(t, x, u) = y\}$, and '$c\ell$' denotes the closure of a set. Furthermore, C is called an invariant control set if $\varphi(t, x, u) \in C$ for all $x \in C$, $u \in \mathcal{U}$, $t \geq 0$, and the domain of attraction $\mathcal{A}(C)$ is defined as $\mathcal{A}(C) = \{x \in M,$ there exists $u \in \mathcal{U}$ and $t \geq 0$ with $\varphi(t, x, u) \in C\}$.

The following theorems characterize some aspects of the qualitative behavior of the stochastic system using properties of the associated control system (6).

1. Theorem. *Consider the regular stochastic system (2) and assume that the associated control system (6) has at most finitely many invariant control sets $C_1 \dots C_n$. Then for each $x \in M$ there exist $n+1$ numbers $p_j(x)$, $p_\infty(x)$, $j = 1 \dots n$, such that*

(i) $p_\infty(x) + \sum_{j=1}^{n} p_j(x) = 1$, $p_j(x) > 0$ *iff* $x \in \mathcal{A}(C_j)$,

(ii) $P\{\psi(t, x, \omega) \to C_j \text{ as } t \to \infty\} = p_j(x)$,

(iii) $P\{\psi(t, x, \omega)$ *leaves every compact set outside of invariant control sets in* M *as* $t \to \infty\} = p_\infty(x)$.

Here $\psi(t, x, \omega)$ denotes the pathwise solutions of (2), and P is the underlying probability measure.

In general, not all invariant control sets of (6) carry stationary solutions of (2). This is true, however, if the invariant control sets are compact, or if the system (2) is restricted to a compact, forward invariant set in M.

2. Corollary. *Assume that the invariant control sets $C_j, j = 1 \dots m$ are compact and that $p_\infty(x) = 0$.*

(i) *On each $N \times C_j$ there exists a unique invariant probability measure ν_j of the pair process $(\eta(t),\ x(t))$ which satisfies the Fokker-Panck equation associated with (2.3). The marginal of ν_j on N is λ, and the marginal of ν_j on M, say μ_j, is the unique invariant distribution of $x(t)$ on C_j with support $\mu_j = C_j$.*

(ii) *For each $x \in M$, $\psi(t, x, \cdot)$ converges in distribution to $\sum_{j=1}^{n} p_j(x)\mu_j$, as $t \to \infty$.*

For each point $x \in M$, Theorem 1. and Corollary 2. characterize the limit behavior of the stochastic system (2), starting at x, once the entrance probabilities $p_j(x)$ and the invariant distributions μ_j are known. Without further assumptions, both quantities can only be obtained via numerical simulations. A little more can be said about the size of $p_j(x)$.

3. Remark. Recall that by Theorem 1.(i)., $p_j(x) > 0$ iff $x \in \mathcal{A}(C_j)$. We call a point $x \in M$ multistable, if there exist indices $j \neq k$ with $p_j(x) > 0$ and $p_k(x) > 0$. The

set of multistable points can be characterized via control theoretic concepts, see Colonius et al. (1995). We define the strict domain of attraction of an invariant control set as

$$\mathcal{A}^s(C) = \{x \in M, x \in \mathcal{A}(C) \text{ and } x \notin \mathcal{A}(D) \text{ for any invariant control set } D \neq C\}. \tag{7}$$

Then it follows under the assumptions of Corollary 2. that $p_j(x) = 1$ iff $x \in \mathcal{A}^s(C_j)$.

The final result in this section concerns the stationary solutions of the stochastic system (2) as they develop around the limit sets of the unperturbed system (1). The appropriate set-up for this idea are the Morse sets of (1) under the inner pair condition. Roughly, the Morse sets of (1) are the isolated components of the union of all limit sets; in particular, isolated limit sets are Morse sets, see Conley (1978) for details. A point $x \in M$ in a Morse set of (1) is called an inner point, if there exist times $S, T > 0$ such that $\varphi(T, x, 0)$ lies in the interior of the orbit of the control system (5) up to time $T + S$, see Colonius and Kliemann (1994a) for details.

4. Theorem. *Consider the regular stochastic system (2) and assume that the unperturbed system (1) has finitely many Morse sets $M_1 \dots M_r$. If all points $x \in \bigcup_{k=1}^{r} M_k$ are inner points, then each Morse set M_k is contained in the interior of some control set D_k of the control system (6). Furthermore, if $\rho > 0$ is sufficiently small, then the maximal Morse sets of (1) are contained in invariant control sets (of the system (6) with range U_ρ), and hence the stationary solutions of the stochastic system (2) form around the maximal Morse sets of (1), i.e. around its attractors.*

5. Remark. (Dependence of stationary solutions on the excitation range U_ρ.)
According to Theorem 4., the stationary solutions of the random system (2) form around the attractors of the nominal system (1), if the excitation range is small. For increasing ρ, the control sets of (6) increase and they may change their type from variant to invariant, and vice versa. If an invariant control set C_ρ for $0 < \rho \leq \rho_1$ becomes variant for $\rho > \rho_1$, then the stationary solution in C_ρ, as described in Corollary 2., disappears for $\rho > \rho_1$. We refer the reader to Colonius and Kliemann (1994b) and Colonius et al. (1995) for various examples of this phenomenon.

6. Remark. (Dependence of stationary solutions on the bifurcation parameter α.)
If the stochastic system depends on a parameter $\alpha \in \mathbb{R}^p$ as in (5), then the structure of control sets of the associated system (6), and hence the stationary solutions of (2), may vary with α. The precise bifurcation scenario for the control system depends on the bifurcation behavior of the unperturbed system (1) locally in α, and on the global dynamical effects introduced by the control vector fields and the control range U_ρ. We refer the reader to Colonius and Kliemann (1994b), Colonius et al. (1992, 1995), and Häckl and Schneider (1994) for various results and examples along these lines.

2.3. COLLAPSE BEHAVIOR OF RANDOM DYNAMICAL SYSTEMS – ANALYTICAL RESULTS

Collapse, or sudden failure, of dynamical systems is indicated by state variables crossing certain thresholds. This leads to the following problem formulation in the set-up introduced above:

Let $L \subset M$ be a compact set with nonvoid interior. For an initial value $x_0 \in M$ denote by $\tau_L(x_0) = \inf\{t \geq 0,\ \psi(t, x_0, \omega) \in L^c\}$ the first exit time from L. ($\psi(t, x_0, \omega)$ denotes again the pathwise solutions of the stochastic system (2).) Note that $\tau_L(x_0)$ is a random variable and a stopping time for the system (2). The failure event with respect to the threshold L is defined as $F(x_0) = \{\omega \in \Omega, \tau_L(x_0, \omega) < \infty\}$, the life time is the exit time $\tau_L(x_0)$, and the failure location is the random variable $H(x_0) = \{x \in M,\ x = \psi(\tau_L(x_0), x_0, \omega)\}$. The failure probability from x_0 is given by $q(x_0) = P\{\tau_L(x_0) < \infty\}$. The following results are mostly concerned with failure probabilities.

7. Theorem. *Consider the regular stochastic system (2) with threshold set L. Then for a point $x_0 \in M$: $q(x_0) = P\{\tau_L(x_0) < \infty\} > 0$ iff $\mathcal{O}^+(x_0) \cap L^c \neq \emptyset$, where again $\mathcal{O}^+(x_0)$ denotes the positive orbit of the control system (6).*

Proof. If $q(x_0) > 0$, then there exists a trajectory $(\eta(t, \omega),\ \psi(t, x_0, \omega))$ of the pair process (2,3) and a time $t_0(\omega)$ such that $(\eta(t_0, \omega),\ \psi(t_0, x_0, \omega)) := (\zeta, y) \in N \times L^c$. Since L is compact, there exists an open neighborhood $V(\zeta, y) \subset N \times L^c$. By continuous dependence of the solutions of (6) on u this means that there is a piecewise constant control $u \in \mathcal{U}$ such that $\varphi(t_0, x_0, u) \in L^c$, which shows that $\mathcal{O}^+(x_0) \cap L^c \neq \emptyset$.

Vice versa, if $\mathcal{O}^+(x_0) \cap L^c \neq \emptyset$, we pick $y \in \mathcal{O}^+(x_0) \cap L^c$ and an open neighborhood $W(y) \subset L^c$. Then there exists a piecewise constant control $u \in \mathcal{U}$ with $\varphi(t_1, x_0, u) \in W(y)$ for some $t_1 < \infty$. By continuous dependence of the solutions of (6) on u, there exists an open neighborhood $\mathcal{V}(u) \subset \mathcal{U}$ such that $\varphi(t_1, x_0, v) \in W(y)$ for all $v \in \mathcal{V}(u)$. The support theorem implies that $P\{\mathcal{V}(u)\} > 0$. Since the trajectories of (2) are continuous, we obtain $P\{\tau_L(x_0) < \infty\} > 0$. □

8. Theorem. *Consider the regular system (2) with threshold set L. Under the conditions of Theorem 1, let $x_0 \in L$ and consider the corresponding probabilities $p_j(x_0)$ of approaching an invariant control set C_j as $t \to \infty$, $j = 1,\dots n$, and the probability $p_\infty(x_0)$ that the system leaves every compact set as in Theorem 1. Then the failure probability $q(x_0)$ from x_0 is*

$$q(x_0) = p_\infty(x_0) + \Sigma p_j(x_0)$$

when the sum is taken over all j with $C_j \cap L^c \neq \emptyset$.

Proof. By Theorem 1. (i) it follows that $q(x_0)$ is bounded above by the expression at the right hand side. Conversely, an invariant control set C_j either carries an invariant measure of the system (2) or it is a transient set for (2). In the first case consider the event $\{\omega \in \Omega,\ \sigma_{C_j}(x_0,\omega) < \infty\}$ where $\sigma_A(x_0,\omega) = \inf\{s \geq 0,\ \psi(s,x_0,\omega) \in A\}$ is the first entrance time of the process into the Borel set A. Then $p_j(x_0) = P\{\sigma_j(x_0) < \infty\}$. In the second case, consider the compact set $C_j \cap L \not\subseteq C_j$. Since the process is transient on C_j, it leaves any compact set in C_j with probability 1, for all initial values in C_j. Hence $p_j(x_0) = P\{\omega \in \Omega,\ \sigma_{C_j}(x_0,\omega) < \infty$ and $\tau_L(x_0,\omega) < \infty\}$. For $j = 1,\dots n$, the considered events and $\{\omega \in \Omega,\ \psi(t,x_0,\omega)$ leaves every compact set outside of invariant control sets as $t \to \infty\}$ are pairwise disjoint and contained in $\{\omega \in \Omega,\ \psi(t,x_0,\omega) \in L^c$ for some $t > 0\}$. Hence $q(x_0) \geq p_\infty(x_0) + \Sigma p_j(x_0)$, where the sum is taken over all j with $C_j \cap L \neq \emptyset$. □

While Theorem 7. characterizes the situations in which the failure probability is positive, Theorem 8. leads to some results on failure with probability 1.

9. Corollary. *Under the assumptions of Theorem 8., let $x_0 \in L$ such that $p_j(x_0) > 0$ implies $C_j \cap L^c \neq \emptyset$. Then $q(x_0) = 1$.*

Proof. The result follows directly from Theorem 8., since $p_\infty(x_0)$ is the probability that the system starting in x_0 is transient. □

Note that the following converse of Corollary 9. is obvious: If $q(x_0) = 1$, then $p_j(x_0) > 0$ implies $C_j \cap L^c \neq \emptyset$. The following direct consequences of the results above are often useful in applications to concrete systems.

10. Corollary. *Consider the set-up of Theorem 8.*

(i) *If the system (6) has no invariant control set contained entirely in L, then $q(x_0) = 1$ for all $x_0 \in L$.*

(ii) *If for an invariant control set $C \subset M$ we have $C \cap L^c \neq \emptyset$, then*

(a) *$q(x_0) > 0$ for all $x_0 \in \mathcal{A}(C)$, and*

(b) *$q(x_0) = 1$ for all $x_0 \in \mathcal{A}^s(C)$, the strict domain of attraction of Cdefined in (7).*

The results above characterize the cases in which the failure probability $q(x_0)$ is 0 or 1. For $q(x_0) \in (0,1)$, numerical algorithms are required to compute its value. Similarly, the statistics of the life time distributions $\tau_L(x_0)$ have to be computed numerically. The following result shows that the expectation of $\tau_L(x_0)$ is finite.

11. Theorem. *Consider the regular system (2) with compact threshold set L. If for all $x_0 \in L$ we have $q(x_0) = 1$, then the expectation $\mathbb{E}\tau_L(x_0)$ of the life time distribution is finite for all $x_0 \in L$.*

Proof. Let $x \in L$. By Theorem 7. $\mathcal{O}^+(x) \cap L^c \neq \emptyset$, and there exist a piecewise constant control $u \in \mathcal{U}$, a neighborhood $\mathcal{V}(u) \subset \mathcal{U}$ and a time $t_x \geq 0$ such that $\varphi(t_x,x,v) \in L^c$ for all $v \in \mathcal{V}(u)$. Since the solutions of (6) depend continuously on the initial value, we find an open neighborhood $A(x)$ such that $\varphi(t_x,y,v) \in L^c$ for all $v \in \mathcal{V}(u)$, all $y \in A(x)$. Hence, by the support theorem $P\{\tau_L(y) > t_x\} \leq 1 - P\{\mathcal{V}(u)\} =: \delta(x,t_x) < 1$ for all $y \in A(x)$. By compactness of L we can find a time $T > 0$ such that $\sup_{x \in L} P\{\tau_L(x) > T\} =: \delta(T) < 1$. Therefore by Dynkin (1965), Lemma 4.3,

$$\mathbb{E}\tau_L(x) \leq \frac{T}{1-\delta(T)} < \infty \quad \text{for all} \quad x \in L.$$

□

If the condition $q(x_0) = 1$ for all $x_0 \in L$ in Theorem 11. is replaced by the weaker assumption $q(x_0) > 0$ for all $x_0 \in L$, then the same proof shows that the conditional life time distributions, conditioned on $\{\tau_L(x_0) < \infty\}$, have finite expectation.

12. Remark. Concerning failure location $H(x_0)$, the following observation is easily proved using the support theorem in the same spirit as above. Note that $H(x_0,\omega) \in \partial L$, the boundary of L, since the trajectories of the stochastic system (2) are continuous. Let $B \subset \partial L$ be a (relatively) open set, then $P\{H(x_0) \in B\} > 0$ iff $\mathcal{O}^+(x_0) \cap B \neq \emptyset$. More detailed information on $H(x_0)$ needs to be obtained from numerical simulations.

We close this section with a few remarks on the dependence of the collapse behavior on the excitation range ρ and the bifurcation parameter α. While the failure probability $q(x_0,\rho)$ need not necessarily increase with increasing ρ (see Section 3. for an example), the life time will decrease with increasing ρ, if $q(x_0,\rho) = 1$. The α-dependence of the failure probability, the life

time, and the failure location is again given by the bifurcation behavior of the control system (6). In particular, change of α may reduce the failure probability (even down to zero), see Section 3. for an example.

2.4. DAMAGE ACCUMULATION IN RANDOM DYNAMICAL SYSTEMS – ANALYTICAL RESULTS

Damage accumulation, or fatigue in dynamical systems is measured by the size of appropriate functionals defined on the state space of the system. As discussed in the introduction, we take the view in this paper that damage inflicted at time t is a function of the location of the state variables at time t, compared to the nominal operating point of the system. This leads to the following problem formulation in the set-up of Section 2.1:

A damage function $f : M \to \mathbb{R}^+$ is a measurable bounded function with compact level sets $\{x \in M, f(x) \leq \gamma\}$ for $\gamma \geq 0$. Usually, f will be 0 at the nominal operating point $x^* \in M$, and f increases with the distance from x^*. (Here distance is with respect to an appropriate metric on the state space M.) A typical example of a damage function on $\mathbb{R}^d$ for a system with stable operating point $x^* \in \mathbb{R}^d$ is

$$(8) \quad f(x) = \gamma \cdot \exp[\delta \|x^* - x\|] - \beta, \ \beta, \gamma, \delta \in \mathbb{R}.$$

If $\beta = \gamma$, then no damage occurs at $x = x^*$.

For a trajectory $\psi(t, x_0, \omega)$ of the stochastic system (2), damage accumulation at time $t \geq 0$ is measured via

$$(9) \qquad F(t, x_0, \omega) = \int_0^t f(\psi(s, x_0, \omega))ds.$$

In this model, failure occurs when $F(t, x_0, \omega) \geq \Lambda$, where Λ is a given damage level. Two kinds of distributions describe damage accumulation: For $t \geq 0$ fixed, $F(t, x_0, \cdot)$ is the damage level at time t; and for $\Lambda \geq 0$ fixed, $H(\Lambda, x_0) := \inf\{t \geq 0, \ F(t, x_0, \omega) = \Lambda\}$ is the damage time at level Λ. (Note that F is a continuous function in t and hence H is well defined for all $\Lambda \geq 0$.) In mathematical terms, H is the exit time of the process $F(t, x_0)$ from the set $[0, \Lambda]$. The following results are concerned with properties of the damage accumulation function F. We will assume that the system lives in a compact, forward invariant set $K \subset M$, since transient behavior will lead to system collapse in realistic situations. Note that continuous damage functions on compact sets K are bounded and measurable.

13. Theorem. *Consider the regular stochastic system (2) with its associated control system (6) in a compact, forward invariant set $K \subset M$.*

Then $P\{\lim_{t\to\infty} F(t, x_0) = \infty\} = \Sigma p_j(x_0)$, where the sum is taken over all j with $p_j(x_0) > 0$ and $\mu_j\{x \in K, f(x) > 0\} > 0$. Here $p_j(x_0)$ is given by Theorem 1. and μ_j denotes the unique invariant measure on the invariant control set C_j of (6) (see Corollary 2.). In particular, $\lim_{t\to\infty} F(t, x_0) = \infty$ w.p.1. iff $\mu_j\{x \in K, \ f(x) > 0\} > 0$ for all j with $p_j(x_0) > 0$.

Proof. Recall first that in K the control system (6) has at least one and at most finitely many invariant control sets, which we denote by $C_1, \ldots C_n$. Thus $\sum_{j=1}^{n} p_j(x_0) = 1$ and hence it suffices to prove the first assertion. Furthermore, it follows that $\{\omega \in \Omega, \ \lim_{t\to\infty} F(t, x_0, \omega) = \infty\} = \bigcup_{i=1}^{n} \{\omega \in \Omega, \ \lim_{t\to\infty} F(t, x_0, \omega) = \infty$ and $\sigma_{C_j}(x_0, \omega) < \infty\}$, where σ_B again denotes the first entrance time into the set B. Note that the union is disjoint and hence

(10)

$$P\{\lim_{t\to\infty} F(t, x_0, \omega) = \infty\} = \sum_j \{\lim_{t\to\infty} F(t, x_0, \omega) = \infty \text{ and } \sigma_{C_j}(x_0, \omega) < \infty\}.$$

The right hand side does not change if summation is taken only over all j with $p_j(x_0) > 0$, since $p_j(x_0) = P\{A_j(x_0)\}$, where $A_j(x_0) = \{\omega \in \Omega, \ \sigma_{C_j}(x_0, \omega) < \infty\}$. Now suppose that $p_j(x_0) > 0$ but $\mu_j\{x \in K, f(x) > 0\} = 0$. By boundedness of f, $F(\sigma_{C_j}(x_0), x_0, \omega) < \infty$ for all $\omega \in A_j(x_0)$. Recall that support $\mu_j = C_j$ and therefore $\mu_j\{x \in K, \ f(x) > 0\} = 0$ implies that $f \equiv 0$ on C_j. Hence $F(\sigma_{C_j}(x_0), x_0, \omega) = \lim_{t\to\infty} F(t, x_0, \omega) < \infty$ for all $\omega \in A_j(x_0)$ and thus it suffices to sum in (10) over all j with $p_j(x_0) > 0$ and $\mu_j\{x \in K, f(x) > 0\} > 0$.

For these j one has that $\lim_{t\to\infty} F(t, x_0, \omega) = \infty$ for all $\omega \in A_j(x_0) \cap \Gamma$, where $\Gamma \subset \Omega$ is the event on which the ergodic theorem holds. Hence $P(\Gamma \cap \{\lim_{t\to\infty} F(t, x_0) = \infty$ and $\sigma_{C_j}(x_0 < \infty)\}) = P(\Gamma \cap A_j(x_0)) = P(A_j(x_0)) = p_j(x_0)$. Hence the assertion follows from (10). □

Theorem 13. says, in particular, that $f(x) > 0$ on some open subset of each invariant control set C_j is sufficient for damage accumulation to increase to ∞ over time from all initial conditions $x_0 \in K$. If the damage function f is zero on some sets C_j, then $\lim_{t\to\infty} F(t, x_0) = \infty$ happens with correspondingly smaller probability. The asymptotic damage accumulation for $t \to \infty$ is described in the next result.

14. Theorem. *Consider the regular stochastic system (2) with its associated control system (6) in a compact, forward invariant set $K \subset M$. Let $x_0 \in C$, one of the invariant control sets of (6). Then the asymptotic damage accumulation rate is*

$$\lim_{t\to\infty} \frac{1}{t} F(t, x_0, \omega) = \int_C f(x)\mu(dx) \quad f.a.x_0 \in C \quad w.p.1,$$

where μ is the unique invariant measure of (2) on C, see Corollary 2.

The proof of Theorem 14. is a simple application of the ergodic theorem to the bounded, hence μ-integrable function f on the invariant set C. Theorem 14. generalizes easily to all $x_0 \in K$ by conditioning on the event $A_j(x_0) = \{\omega \in \Omega, \sigma_{C_j}(x_0 < \infty\}$ if $P\{A_j(x_0)\} = p_j(x_0) > 0$. Finally, we have a result on the expectation of the damage time $H(\Lambda, x_0)$, which can be proved along the lines of Theorem 11.

15. Theorem. *Under the assumptions of Theorem 13., assume that $\lim_{t\to\infty} F(t, x_0) = \infty$ w.p.l. Then for each $\Lambda \geq 0$ the expectation $\mathbb{E}H(\Lambda, x_0)$ of the damage time at level Λ is finite.*

3. COLLAPSE AND DAMAGE ACCUMULATION IN THE TAKENS-BOGDANOV OSCILLATOR WITH EXTERNAL EXCITATION

3.1. THE TAKENS-BOGDANOV OSCILLATOR WITH EXTERNAL EXCITATION

Mathematically, the Takens-Bogdanov oscillator represents the simplest case of a codimension two bifurcation. Its universal unfolding exhibits stationary, Hopf, and homoclinic bifurcations. This system occurs as a model e.g. for the motion of a thin panel in a flow, for shock waves, population dynamics, or solar gravity.

The Takens-Bogdanov oscillator is given by the two-dimensional differential equation

$$\begin{aligned} \dot{x} &= y \\ \dot{y} &= \lambda_1 + \lambda_2 x + x^2 + xy, \end{aligned} \tag{11}$$

with bifurcation parameter $(\lambda_1, \lambda_2) \in \mathbb{R}^2$. We are interested in the reliability behavior of (1) under external excitation, i.e. we consider

$$\begin{aligned} \dot{x} &= y \\ \dot{y} &= \lambda_1 + \lambda_2 x + x^2 + xy + \xi(t), \end{aligned} \tag{12}$$

where $\xi(t) = f_\rho(\eta(t))$, with $\eta(t)$ a diffusion process satisfying the conditions of Section 2.1. We denote the excitation range by

$$U_\rho = [-\rho, \rho] \subset \mathbb{R}. \tag{13}$$

This system is regular, i.e. it satisfies Assumption (H) from Section 2.2. For a discussion of system (11) and of the control system associated with (12) we refer the reader to Häckl and Schneider (1994).

For the ensuing reliability analysis, we use the following set-up:

- $(\lambda_1, \lambda_2) = (-0.3, -1)$. For these values the unperturbed system (1) has a stable focus E_F and a hyperbolic saddle point E_S.
- The background noise $\eta(t)$ is the Wiener process on the one-dimensional sphere $\mathbb{S}^1$.
- $f_\rho : \mathbb{S}^1 \to [-\rho, \rho]$, $f_\rho(\eta) = \rho \cdot \sin\eta$ maps the background noise $\eta(t)$ onto the external excitation $\xi(t)$ in U_ρ.

For our numerical results, we simulate 'true' trajectories of the Wiener process by using normally distributed increments of this process on $\mathbb{R}$ and by identifying the points $2n\pi$, $n \in \mathbb{Z}$. With the corresponding trajectories of $\xi(t)$, the equation (12) is then integrated using a fifth order Runge-Kutta scheme, see Kloeden and Platen (1992) for details on numerical solutions of stochastic differential equations. Computation of control sets, multistability regions, and domains of attraction for the associated control system is based on numerical computation of orbits as described in Häckl (1993).

3.2. COLLAPSE IN THE TAKENS-BOGDANOV OSCILLATOR

In order to study collapse phenomena in the Takens-Bogdanov oscillator, we considered excitation ranges $\rho \in [0, 0.3]$ and define the threshold set to be

$$L = [-1.5, 1.5] \times [-100, 100] \subset \mathbb{R}^2. \tag{14}$$

For the initial value we chose the stable operating point E_F (stable focus) of the unperturbed system (11) (except when different initial values are mentioned explicitly). For this initial value and noise ranges, the threshold set (14) guarantees that the position variable x is the restricting variable, indicating system collapse due to excessive dislocation. Figure 1. shows the phase portrait of the unperturbed system. The unstable manifold of the hyperbolic saddle E_S approaches the stable focus E_F. We remark that in the noise range specified above there are (constant) parameter values $(\lambda_1 + \xi, \lambda_2)$ such that the corresponding hyperbolic saddle E_S possesses a homoclinic orbit. Hence the excited equation 'mixes' dynamical behavior of considerable complexity.

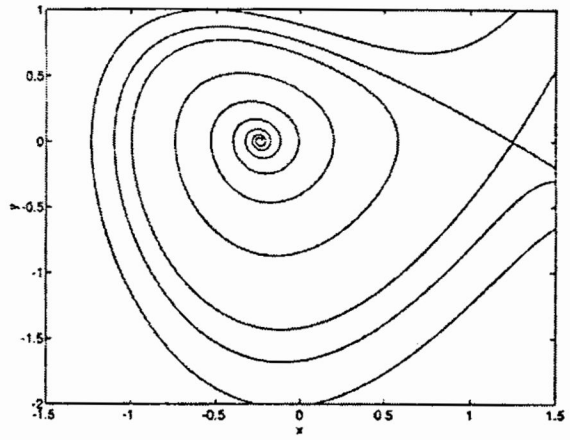

Figure 1. Phase portrait of the Takens-Bogdanov oscillator (unperturbed).

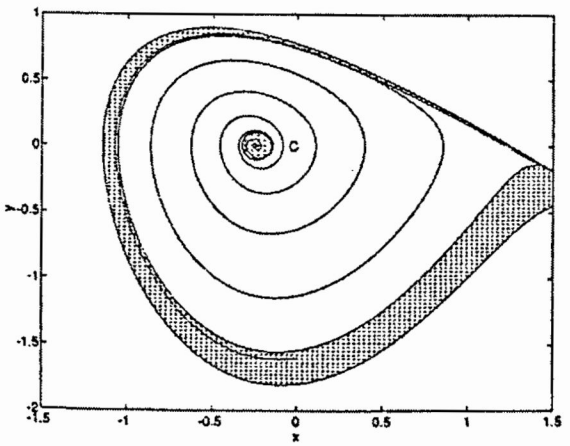

Figure 2. Invariant control set C and bistability region, $\rho = 0.02$.

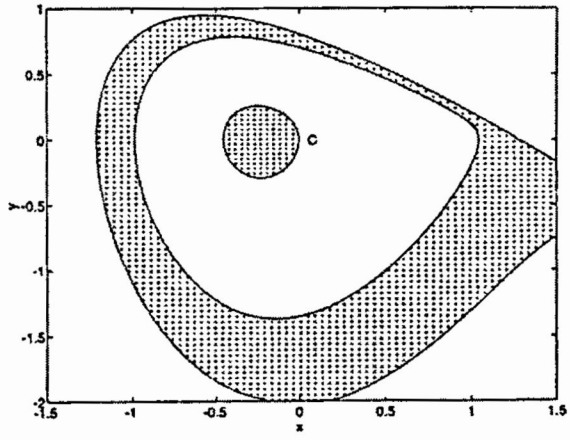

Figure 3. Invariant control set C and bistability region, $\rho = 0.05$.

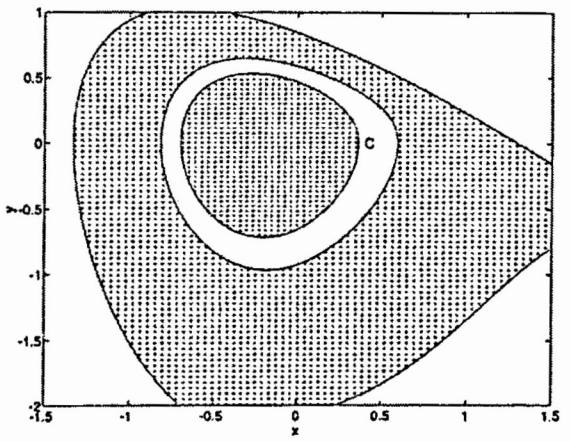

Figure 4. Invariant control set C bistability region, $\rho = 0.09$.

3.2.1. FAILURE PROBABILITIES

Recall that the failure probability of a random system from the point (x_0, y_0) is defined as $q(x_0, y_0) = P\{\tau_L(x_0, y_0) < \infty\}$, i.e. as the probability that the system exists the threshold set L in finite time. According to Theorems 8., 9. and Corollaries 10., 11. the size of the failure probabilities can be estimated by considering the control sets and their domains of attraction for the associated control system. According to Theorem 4. the invariant control sets develop around the stable attractors of the unperturbed system.

Figures 2.-4. show the invariant control sets C_ρ around the stable focus E_F (shaded areas in the center), and the bistability regions (shaded anulus-type regions) for $\rho = 0.02, 0.05, 0.09$. In this case, the bistability region is given by a variant (i.e. not invariant) control set and its domain of attraction. Then the strict domain of attraction $\mathcal{A}^s(C_\rho)$ is the domain bounded by the inner boundary of the bistability region, the domain of attraction $\mathcal{A}(C_\rho)$ is the domain bounded by its outer boundary. Figure 2. also shows a simulated trajectory. For $\rho = 0.1$ the invariant and the variant control set have merged into one variant control set as shown in Figure 5. A bifurcation of control sets has occurred for $\rho \in [0.09, 0.1]$. Figure 6. shows the boundaries of the invariant control sets for $\rho = 0.03, 0.05, 0.07, 0.09$, and ρ_c. For $\rho > \rho_c$, no invariant control set exists. Numerically we compute $\rho_c \in [0.0923, 0.0924]$.

Based on these results the failure probabilities for initial values in L depend on the excitation range ρ in

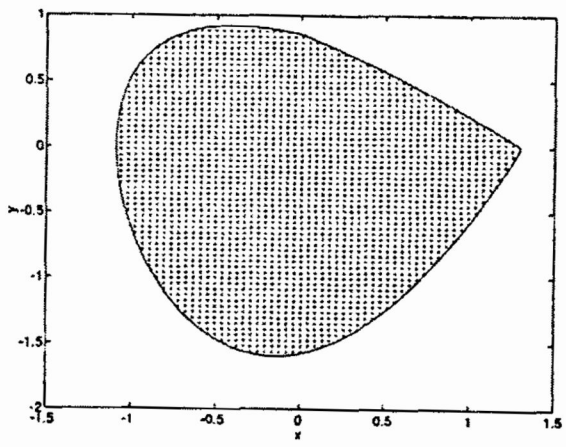

Figure 5. Variant control set, $\rho = 0.1$.

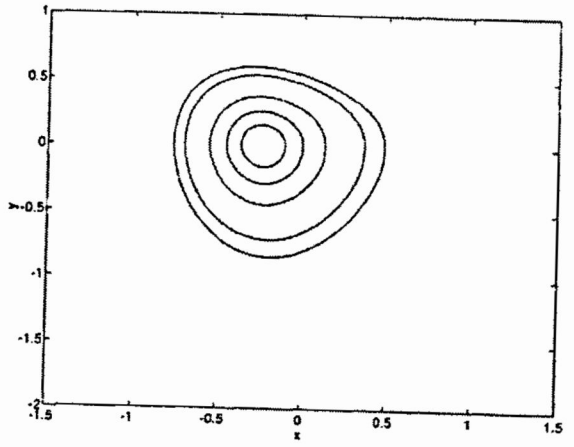

Figure 6. Boundaries of the invariant control set, $\rho = 0.03, 0.05, 0.07, 0.09, 0.0923$.

the following way:

- $(x_0, y_0) \in C_{\rho_c} : q(x_0, y_0) = 0$ for $\rho \leq \rho_c, q(x_0, y_0) = 1$ for $\rho > \rho_c$.
- $(x_0, y_0) \in \mathcal{A}(E_F) \setminus C_{\rho_c}$ where $\mathcal{A}(E_F)$ is the domain of attraction of E_F in the unperturbed system : $q(x_0, y_0) = 0$ for ρ with $(x_0, y_0) \in \mathcal{A}^s(C_\rho)$
  $q(x_0, y_0) > 0$ for $\rho \leq \rho_c$, $(x_0, y_0) \in \mathcal{A}(C_\rho)$
  $q(x_0, y_0) = 1$ for $\rho > \rho_c$
- $(x_0, y_0) \in \mathcal{A}(C_{\rho_c} \setminus \mathcal{A}(E_F) : q(x_0, y_0) = 1$ for ρ with $(x_0, y_0) \notin \mathcal{A}(C_\rho)$
  $q(x_0, y_0) < 1$ for ρ with $(x_0, y_0) \in \mathcal{A}(C_\rho)$
  $q(x_0, y_0) = 1$ for $\rho > \rho_c$
- $(x_0, y_0) \notin \mathcal{A}(C_{\rho_c} : q(x_0, y_0) = 1$ for all $\rho \geq 0$.

Note that control sets and their domains of attracton increase with ρ, and hence these four cases are the only ones possible. The only surprising observation may be the third case: Here the failure probability decreases with increasing excitation range on a certain ρ-interval, before it increases, again to 1. The first case shows abrupt change in failure behavior, as $q(x_0, y_0)$ jumps from 0 to 1 at $\rho = \rho_c$. This case includes the initial value E_F, the stable focus. We will analyze the life time and failure location for this point in the next sections.

Before we leave this section, we mention briefly the dependence of the failure probability $q(x_0, y_0)$ on the bifurcation parameter (λ_1, λ_2). The Takens-Bogdanov oscillator (11) is a special case of the parameter dependent system (5). The following comments are based on the computation of invariant control sets in Häckl and Schneider (1994). Consider the initial value $(x_0, y_0) = (0, 0)$, then

- for $\lambda = (-0.1, -1), \rho = 0.04 : q(0, 0) = 1$
- for $\lambda = (-0.213605, -1), \rho = 0.05 : q(0, 0) = 0$
  $\rho = 0.07 : q(0, 0) = 1$
- for $\lambda = (-0.3, -1), \rho = 0.09 : q(0, 0) = 0$
  $\rho = 0.1 : q(0, 0) = 1$.

If λ_1 is a design parameter of the system, which can be adjusted within the interval $[-0.3, -0.1]$, then the setting $\lambda_1 = -0.3$ guarantees optimal robustness of the system with respect to failure probabilities (at the threshold set L in (14)). In particular, if the excitation range satisfies $\rho \leq \rho_c$, then at this parameter setting failure will not occur with probability one.

3.2.2. LIFE TIME DISTRIBUTIONS, OR EXIT TIMES FROM THRESHOLD SETS

In this section we analyze the life time distributions of the Takens-Bogdonov oscillator for various excitation ranges. Mathematically, the life time of a system is its first exit time from a threshold set L, denoted here by $\tau(\rho)$. This quantity depends on the set L (see (4)), the initial value (taken to be the stable focus E_F), the excitation range ρ, and the dynamics of the excitation (compare Section 3.1.). We will concentrate on the dependence on ρ for $\rho > \rho_c$, where ρ_c was given in the previous section. In this case the expectation $\mathbb{E}\tau(\rho)$ exists for all $\rho > \rho_c$ by Theorem 11. For the system under consideration, there is no analytical method that gives explicit expressions for the life time distribution or its moments. Therefore we conducted a series of numerical simulations, where we set the maximal simulation time for a trajectory to $T = 2000$.

Recall from the previous section that $\rho_c \in [0.0923, 0.024]$. In general, $\tau(\rho)$ will decrease for increasing $\rho > \rho_c$, and it should be 'rather large' for ρ close to ρ_c.

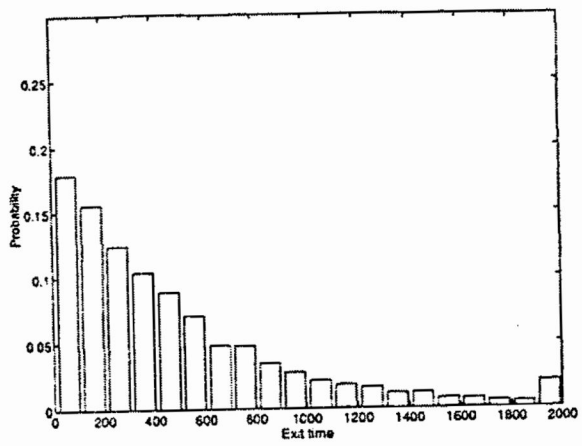

Figure 7. Lifetime distribution, $\rho = 0.25$, time interval $[0, 2000]$.

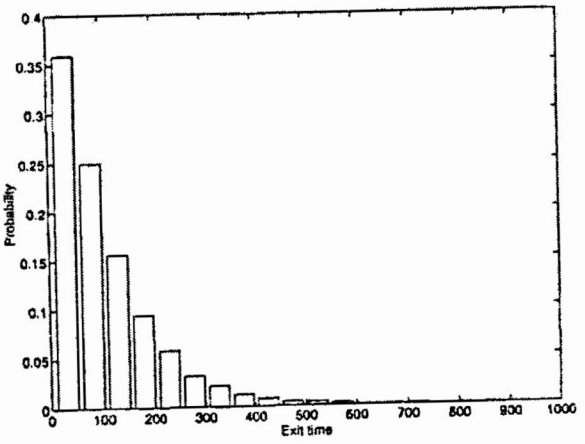

Figure 9. Lifetime distribution, $\rho = 0.3$, time interval $[0, 1000]$.

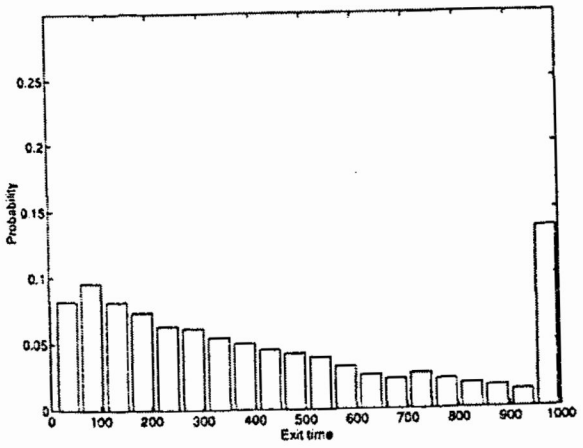

Figure 8. Lifetime distribution, $\rho = 0.25$, time interval $[0, 1000]$.

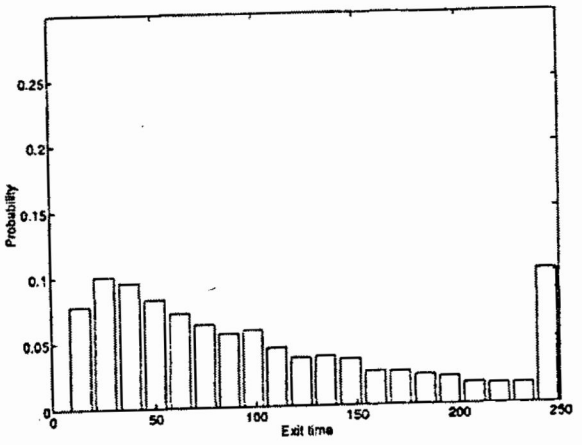

Figure 10. Lifetime distribution, $\rho = 0.3$ time interval $[0, 250]$.

For $\rho = 0.2$ the simulations result in about 14% of the trajectories exiting L before time $T = 2000$, and 8% exiting before time 1000. The reason for this low exit rate is easily understood: For initial values in C_{ρ_c}, the boundary ∂C_{ρ_c} of the maximal invariant control set acts as an exit barrier (see Figure 6.). Only trajectories that are close to this barrier and that experience excitation above the level ρ_c can exit through the barrier. (Compare also the invariant distributions of the system for $\rho < \rho_c$, e.g. Figure 20. for $\rho = 0.05$.) As $\rho > \rho_c$ increases, crossings of ∂C_{ρ_c} occur with higher probability. Hence for ρ close to ρ_c the system is still 'practically stable' in the sense that exit times from L are so large that collapse does not occur within a 'reasonable' time horizon. For $\rho = 0.1$, none of the simulated 200 trajectories left C_{ρ_c} before $T = 2000$.

In applications, crossing of the exit barrier C_{ρ_c} can also serve as an 'early warning signal': For $\rho > \rho_c$ the system has one variant control set D_ρ (see Figure 5. for $\rho = 0.1$) which contains C_{ρ_c} in its interior. From any point in the domain of attraction $\mathcal{A}(D_\rho)$ there is a positive probability that the system will return to a neighborhood of the stable focus E_F. However, this probability is relatively small for trajectories that have crossed the exit barrier. Therefore, although the time for actual collapse may be much larger than the crossing time of ∂C_{ρ_c}, collapse will occur with high probability once the system exits through the barrier.

Figures 7. and 8. show the life time distribution of the system for excitation level $\rho = 0.25$ based on 5000 simulations with different maximal exit times. The mean exit time is $m(\rho = 0.25) = 481.42$. For $\rho = 0.3$ the life time distribution is shown in Figures 9. and 10., again based on 5000 simulations. Here $m(\rho = 0.3)$

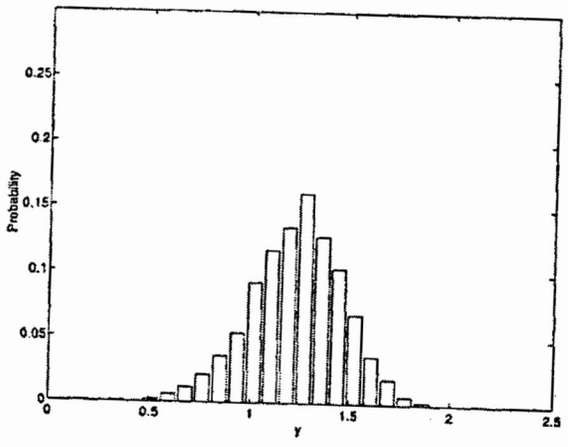

Figure 11. Failure location at boundary $x = 1.5$, $\rho = 0.25$.

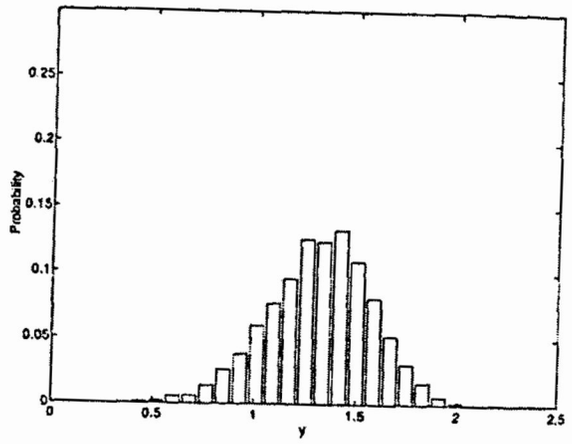

Figure 12. Failure location at boundary $x = 1.5$, $\rho = 0.3$.

$= 112.17$. Both distributions are unimodal, with mode much smaller than the mean, and with heavy right hand tails. The modes in Figures 8. and 10. occur in the second bar illustrating that the system needs a certain time before it collapses since the starting point of all simulated trajectories is the stable focus E_F.

3.2.3. FAILURE LOCATION

Failure location of a random system at the threshold set is given by the random variable $H = \{x \in M,\ x = \psi(\tau_L(x_0, y_0),\ (x_0, y_0), \omega)\}$ i.e. by the point at which the trajectory ψ exists the threshold set. This variable depends on the same quantities as the life time distribution, and we will present some results for $H(\rho)$ depending on the excitation range. Recall that by Remark 12. the maximal possible exit set can be obtained by computing the corresponding orbit of the associated control system.

For excitation range $\rho = 0.25$, 98.8% of the failures occurred at the right boundary $\{1.5\} \times [-100, 100]$. The failure location distribution for this boundary is shown in Figure 11. For $\rho = 0.3$, all trajectories exit at the right boundary. The corresponding failure location distribution is shown in Figure 12. Both figures are based on 5000 simulations. As expected, Figure 12. shows a slight shift to larger values when compared to Figure 11., since increased excitation affects the velocity component of the system (12).

3.3. DAMAGE ACCUMULATION IN THE TAKENS-BAGDANOV OSCILLATOR

In this section we analyze damage accumulation in the Takens-Bogdanov oscillator as it occurs during (small) vibrations around the nominal operating point due to external excitation. We consider the system (12) with excitation range $\rho \in [0, 0.09]$. The damage function is given by

$$f(x, y) = \exp[\delta \| E_F - (x, y) \|], \ \delta = 0.25. \tag{15}$$

Here E_F is the stable focus of the undisturbed system, see Figure 1. Recall that by the results in Section 3.2.1., the associated control system has one invariant control set C_ρ for all $\rho \in [0, 0.09]$, which contains the point E_F in its interior, see Figures 2.-4. Hence by Corollary 2. the system has a unique invariant distribution μ_ρ in this control set, and according to the law of large numbers each solution in C_ρ converges in distribution to μ_ρ as $t \to \infty$.

We present the results of a series of simulations using the numerical schemes described in Section 3.1. with 5000 trajectories.

The distribution of the damage accumulation $F(t, E_F, \omega)$ (see Equation (9)) is shown in Figures 13.-16. for $t \in [0, 100]$ and $\rho = 0.03, 0.05, 0.07$, and 0.09. As expected, the damage accumulation increases for increasing ρ, and the distributions have a wider spread. The distributions show, as functions of t, an oscillatory component. This is due to the fact that the vectorfield is not symmetric around the focus E_F, while the damage function f in (15) has circular level sets around E_F. Figure 17. is a plot of the modes of the distributions against time. It shows this oscillatory behavior, which is reduced for larger ρ-values due to better mixing of the process.

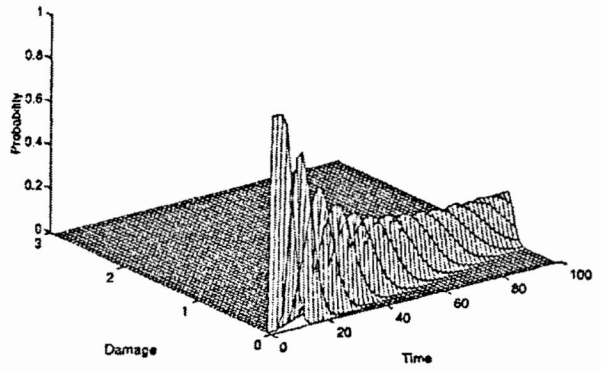

Figure 13. Distribution of damage accumulation, $\rho = 0.03$.

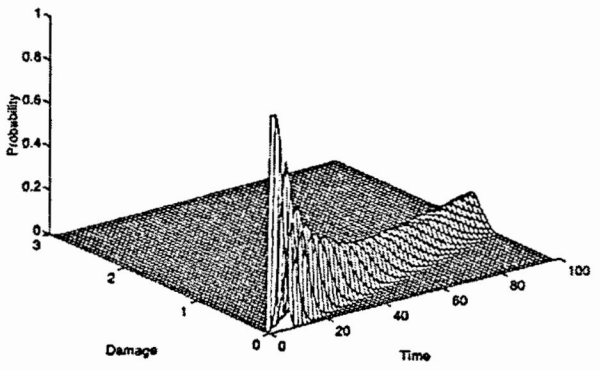

Figure 14. Distribution of damage accumulation, $\rho = 0.05$.

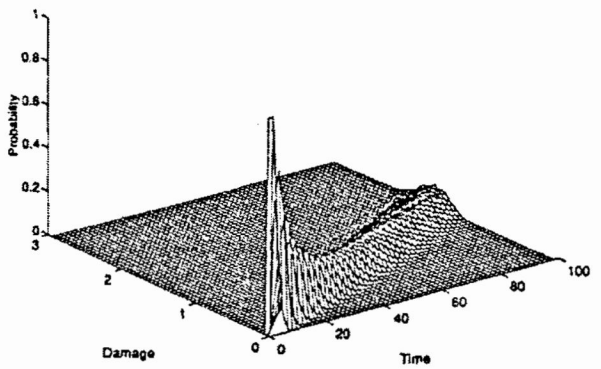

Figure 15. Distribution of damage accumulation, $\rho = 0.07$.

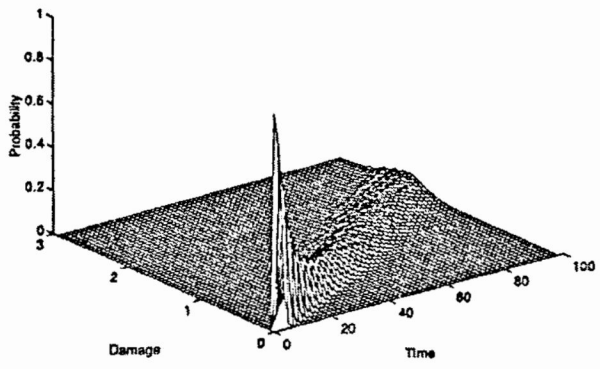

Figure 16. Distribution of damage accumulation, $\rho = 0.09$.

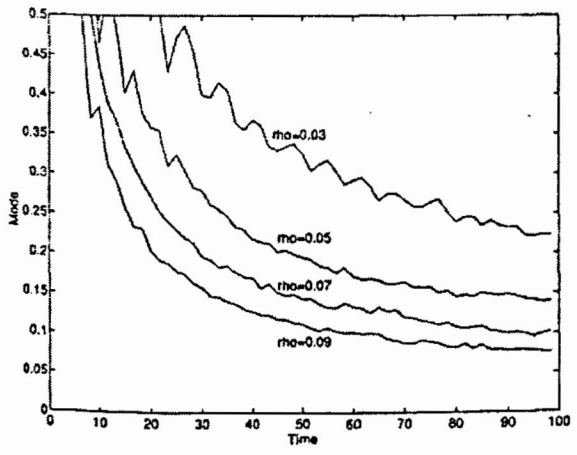

Figure 17. Modes of the damage accumulation distribution, $\rho = 0.03, 0.05, 0.07, 0.09$.

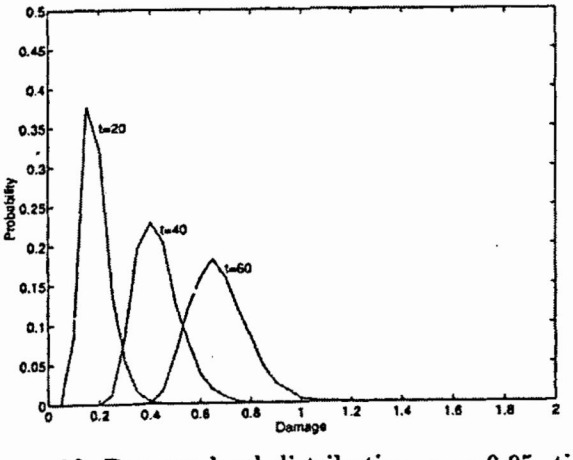

Figure 18. Damage level distribution, $\rho = 0.05$, time $t = 20, 40, 60$.

The distribution of the damage level $F(t_0, E_F)$ at time t_0 is the cross section of the damage accumulation distributions at the time t_0. For $\rho = 0.05$ and $t_0 = 20, 40, 60$ the damage distributions are shown in Figure 18. These damage distributions provide answers to the following question: Given a damage level Λ and a time horizon T, what is the probability that the system has reached the level Λ up to time T? The answer is the corresponding percentile of the damage distribution at time T.

The damage time $H(\Lambda, E_F)$ at level Λ is the cross section of the damage accumulation distributions at the level Λ. For $\rho = 0.05$ and $\Lambda = 0.3, 0.6, 0.9$ the damage time distributions are shown in Figure 19. Note that the damage time distributions are fairly symmetric, while the damage level distributions are skewed to smaller damage levels.

The asymptotic damage accumulation rate (see Theorem 14.)

$$(16) \quad R(\rho) = \lim_{t\to\infty} \frac{1}{t} F(t, (x_0, y_0), \omega) = \int_{C_\rho} f(x)\mu_\rho(dx)$$

is, for each $\rho \geq 0$, a constant w.p.1, independent of the initial value $(x_0, y_0) \in C_\rho$. The invariant distributions μ_ρ on C_ρ were obtained via the simulation of a trajectory up to time 500,000, for $\rho = 0.03, 0.05, 0.07, 0.09$ (compare Kloeden and Platen (1992) for details on the numerical computation of invariant measures via simulation of trajectories). As an example, the corresponding density for $\rho = 0.05$ is shown in Figure 20. The exact support of the invariant density is the corresponding control set, indicated by a drop in the grid of Figure 20. The asymptotic damage accumulation rate is then obtained by numerically integrating the damage function f in (15) with respect to μ_ρ. Numerical evaluation of (16) in this way depends on a variety of factors, such as grid size for the computation of μ_ρ (we used a grid of size 40×40 on the smallest rectangle containing C_ρ), evaluation of f on the grid (we used the minimum and the maximum of f on each cell for comparison), on the numerical stochastic integration scheme for Equation (12) (our fifth order Runge-Kutta scheme emphasizes the tails of μ_ρ more than e.g. an Euler scheme with same step size), and on other factors. The results are given in Table 1., columns 2 and 3. As a comparison, computation of the invariant measure μ_ρ for $\rho = 0.03$ via an Euler scheme results in an interval for $R(0.03)$ of $[0,0071, 0.0085]$, as compared to $[0.0075, 0.0089]$ via the Runge-Kutta scheme. Since the damage function f increases exponentially with the distance from the stable focus E_F, underestimation of the tails of μ_ρ result in smaller values of $R(\rho)$.

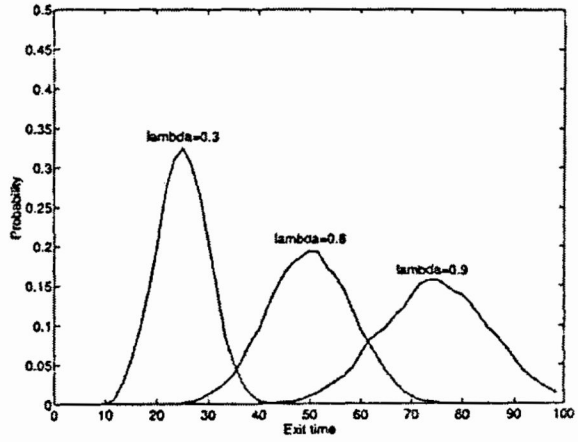

Figure 19. Damage time distribution, $\rho = 0.05$, level $\Lambda = 0.3, 0.6, 0.9$.

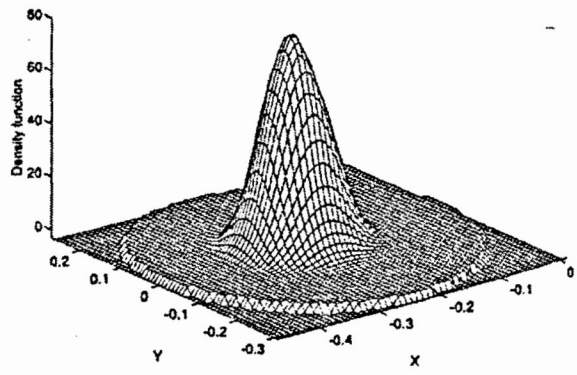

Figure 20. Invariant density, $\rho = 0.05$, support indicated by drop in grid.

A finite time approximation of the damage accumulation rate at time t_o can also be obtained as

$$(17) \quad R(\rho, t_0) = \mathbb{E}\{\frac{1}{t_0} F(t_0, E_F, \omega)\}, \; t_0 \geq 0.$$

Again, the numerical evaluation of (17) depends on several factors, such as the integration scheme used to solve Equation (12), the grid size used for recording the damage accumulation in form of Figures 13.-16., evaluation of f on this grid, the initial value in C_ρ, the time t_0, and other factors. We used the algorithm leading to Figures 13.-16. at time $t_0 = 100$ (with 5000 trajectories). Due to the (constant) initial value E_F and the time restriction $t_0 = 100$, this procedure will underestimate the tails, and hence results in smaller values for the damage accumulation rate. The results

DAMAGE ACCUMULATION RATE R(ρ)

excitation range	via invariant measure		via finite time expectation	
	min f	max f	min f	max f
0.03	.0075	.0089	.0066	.0073
0.05	.0122	.0150	.0113	.0120
0.07	.0173	.0209	.0161	.0168
0.09	.0222	.0270	.0209	.0217

Table 1. Numerical computation of the damage accumulation rate R(ρ).

are given in Table 1., columns 4 and 5, again for f evaluated as the minimum, and the maximum on each cell. As expected, computing the invariant measures μ_ρ via a higher order scheme and using the maximum of f on each cell results in a conservative upper bound for the damage accumulation rate $R(\rho)$. As a consequence we note that computing the damage accumulation rate via the invariant measure is preferable to computing it via finite time expectation.

4. COLLAPSE IN A MODEL FOR SHIP ROLL MOTION

4.1. A MODEL FOR SHIP ROLL MOTION

Capsizing of vessels in random seas can be modelled by a one degree of freedom system which is limited to the roll motion. We refer in particular to Hsieh et al. (1994) (see also Falzarano et al. (1992) and Thompson et al. (1993)). The model in non-dimensionalized form is

$$\begin{aligned} \dot{x} &= y \\ \dot{y} &= -x + \alpha x^3 - \delta_1 y - \delta_2 y|y| + \xi(t) \end{aligned} \tag{18}$$

where $\delta_1 > 0$ and $\delta_2 > 0$ represent the linear and quadratic viscous damping coefficients, respectively, and α denotes the strength of the nonlinearity. The external excitation from waves is modelled via $\xi(t)$. We take $\xi(t)$ as a bounded noise coming from an underlying diffusion $\eta(t)$ as described in Section 2.1. Possible choices for $\eta(t)$ are e.g. white noise on the unit circle $\mathbb{S}^1$ or an Ornstein-Uhlenbeck process $\dot{\eta} = -a\eta + bdW$, where a and b can be adjusted to obtain a certain spectrum.

Capsizing occurs when $|x|$ exceeds $\frac{1}{\sqrt{\alpha}}$.

As in Section 3. we take $\xi(t) = f_\rho(\eta(t))$ and $U_\rho = [-\rho, \rho]$. The system is regular, i.e. it satisfies Assumption (H) from Section 2.2.

For the ensuing reliability analysis, we use the following set-up:

- $\alpha = 1$, the viscous damping coefficients δ_1, δ_2 are given by $\delta_1 = \delta_2 = 1.0$;
- the underlying diffusion process η is taken as a Wiener process on the unit sphere $\mathbb{S}^1$;
- $f_\rho : \mathbb{S}^1 \to [-\rho, \rho]$, $f_\rho(\eta) = \rho \cdot \sin\eta$ maps the background noise $\eta(t)$ onto the external excitation $\xi(t)$ in U_ρ.

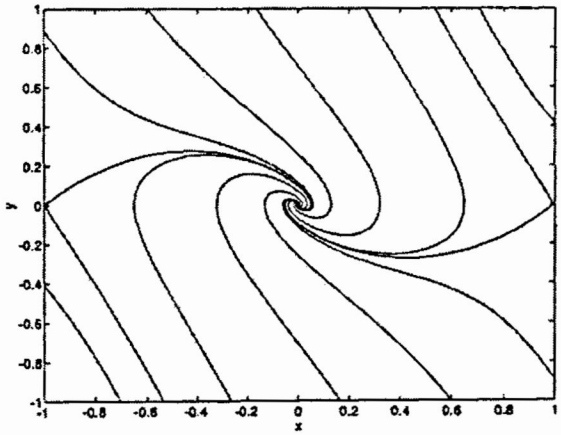

Figure 21. Phase portrait of the ship roll model (unperturbed).

4.2. COLLAPSE IN THE SHIP ROLL MODEL

In the ship roll model collapse, i.e. capsizing, occurs when $|x| > \frac{1}{\sqrt{\alpha}}$. Hence we define the threshold set to be

$$L = [-1, 1] \times [-100, 100]$$

Figure 21. shows the phase portrait of the unperturbed system. It has a stable equilibrium at the origin and two hyperbolic equilibria at $(x, y) = \left(\pm\frac{1}{\sqrt{\alpha}}, 0\right)$. For the chosen parameter values the unstable manifolds of these equilibria form a symmetric pair of heteroclinic orbits connecting them to the stable equilibrium at the origin.

4.2.1. FAILURE PROBABILITIES

We proceed as in the analysis of the Takens-Bogdanov oscillator. Figure 22. shows the invariant control set C_ρ for $\rho = 0.3$, which develops around the stable equilibrium at the origin, and the two bistability regions. They are given by variant control sets which develop around the two hyperbolic equilibria and their respective domains of attraction. The strict domain of attraction $\mathcal{A}^s(C_\rho)$ is given by the region bounded by the inner boundaries of the bistability regions, the domain of attraction $\mathcal{A}(C_\rho)$ is the region bounded by the outer boundaries. A bifurcation of control sets occurs at $\rho = \rho_c$, where all three control sets merge into one variant control set. Numerically we compute $\rho_c \in [0.3849, 0.3850]$. Figure 23. shows the boundaries

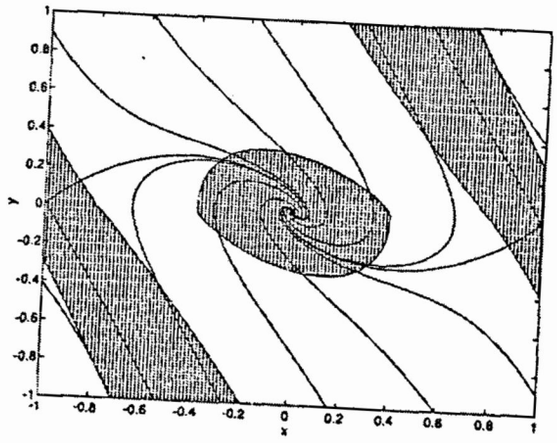

Figure 22. Invariant control set and bistability region, $\rho = 0.3$.

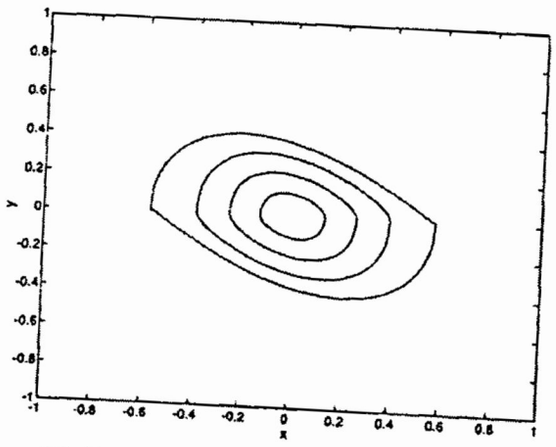

Figure 23. Boundaries of the invariant control set, $\rho = 0.1, 0.2, 0.3, 0.3849$.

of the invariant control sets for different ρ-values up to $\rho = \rho_c$.

Based on these results the failure probabilities for initial values in L depend on the excitation range in a way, which is completely analogous to the discussion in Section 3.2.1. for the Takens- Bogdanov oscillator. Hence we omit the details.

4.2.2. LIFE TIME DISTRIBUTIONS OR EXIT TIMES FROM THRESHOLD SETS

In this section we briefly discuss a series of numerical simulations in order to compute the life time distributions, i.e. the first exit times from the threshold set L. We concentrate on the dependence on ρ for $\rho > \rho_c$, where ρ_c is the critical ρ-value where the invariant controls et and the bistability regions merge, hence the failure probability is $q(x_0, y_0) = 1$ for $\rho > \rho_c$. Recall that $\rho_c \in [0.3849, 0.3850]$. Figures 24.-28. show the

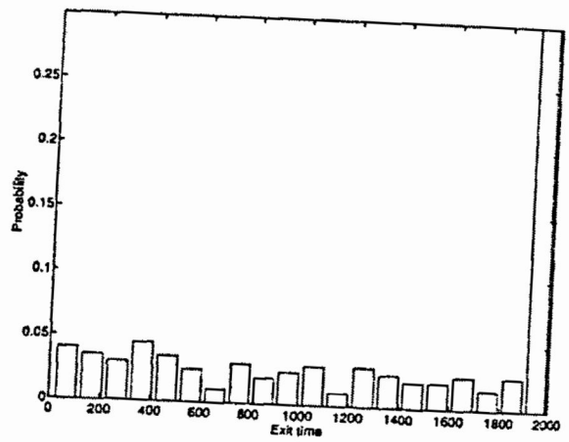

Figure 24. Lifetime distribution, $\rho = 0.5$, time interval $[0, 2000]$.

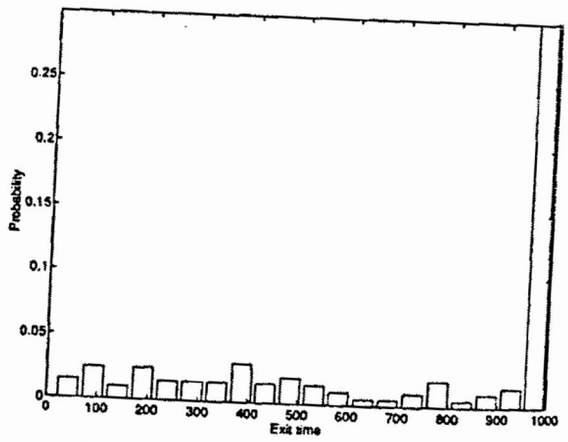

Figure 25. Lifetime distribution, $\rho = 0.5$, time interval $[0, 1000]$.

exit times from the origin for $\rho = 0.5, 0.7, 0.9$ with different maximal exit times. Again the boundary of the invariant control set C_{ρ_c} acts as an exit barrier and in Figure 24. an oscillatory behavior can be observed for $\rho = 0.5$. The mean exit time is 1432.08. This is based on 200 experiments, while the exit time distributions for $\rho = 0.7, 0.9$ in Figure 26.-28. are based on 5000 experiments. Here the mean is 33.20 and 13.75, respectively.

4.2.3. FAILURE LOCATION

The failure location is given by the random variable $H = \{x \in M,\ x = \psi(\tau_L(x_0, y_0), (x_0, y_0), \omega)\}$, i.e. by the point at which the trajectory exits the threshold set.

For excitation range $\rho = 0.7$ and 0.9 the exit locations (again from the origin) at the right boundary $x = 1.0$ and the left boundary $x = -1.0$ are shown in

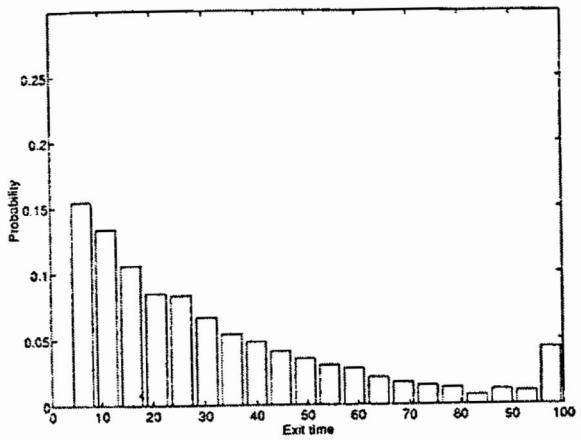

Figure 26. Lifetime distribution, $\rho = 0.7$, time interval $[0, 100]$.

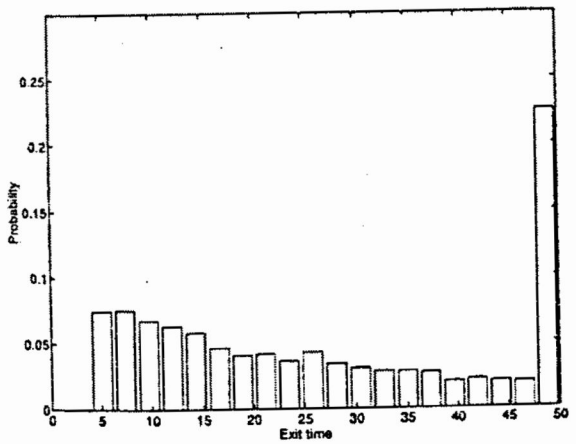

Figure 27. Lifetime distribution, $\rho = 0.7$, time interval $[0, 50]$.

Figures 29.-31. The probabilities of hitting the right and the left boundary (within the maximal exit time 2000) are 0.5, respectively. The exit locations for the two boundaries are symmetric with respect to each other, which may perhaps be expected due to the symmetry of the underlying differential equation. Note, however, that the random excitations acting on the system do not lead to symmetric trajectories.

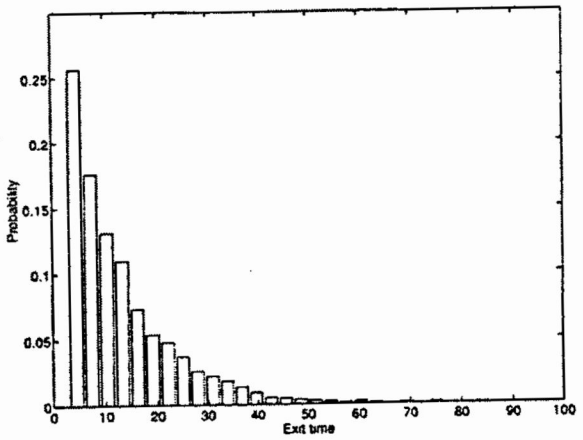

Figure 28. Lifetime distribution, $\rho = 0.9$, time interval $[0, 100]$.

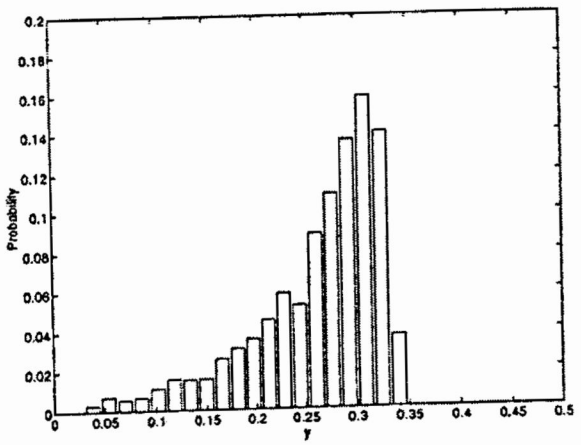

Figure 29. Failure location at boundary $x = 1.0$, $\rho = 0.7$.

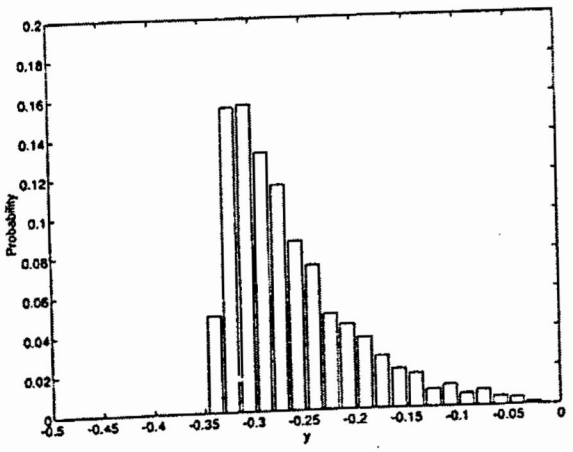

Figure 30. Failure location at boundary $x = -1.0$, $\rho = 0.7$.

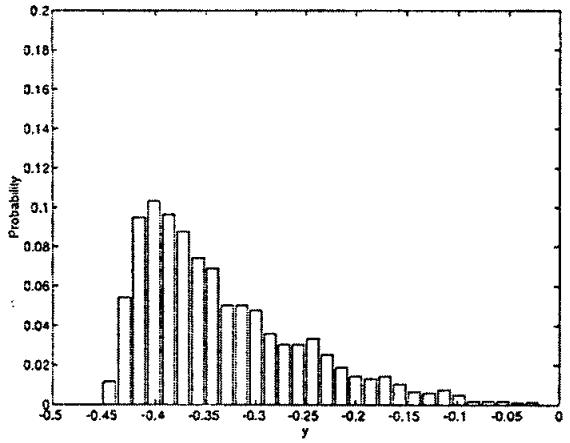

Figure 31. Failure location at boundary $x = -1.0$, $\rho = 0.9$.

REFERENCES

Bolotin, V.V., 1995, "Fatigue crack propagation in random media," Nonlinear Dynamics and Stochastic Mechanics, W. Kliemann, N.S. Namachchivaya (eds.), CRC Press, Boca Raton, 361–381.

Barlow, R.E., Proschan, F., 1975, "Statistical Theory of Reliability and Life Testing," Holt, Rinehart and Winston, New York.

Conley, C., 1978, "Isolated Invariant Sets and the Morse Index," CBMS Regional Conference Series, no. 38, American Mathematical Society, Providence.

Colonius, F., Kliemann, W., 1993, "Some aspects of control systems as dynamical systems," J. Dynamics Diff. Equations, Vol. 5, 469–494.

Colonius, F., Kliemann, W., 1994a, "Limit behavior and genericity for nonlinear control systems," Differential Equations, Vol 109, 8–41.

Colonius, F., Kliemann, W., 1994b, "Random perturbations of bifurcation diagrams," Nonlinear Dynamics, Vol 5, 353–373.

Colonius, F., De La Rubia, F.J., Kliemann, W., 1995, "Stochastic models with multistability and extinction levels," to appear in SIAM J Appl Math.

Colonius, F., Häckl, G., Kliemann, W., 1992, "Controllability near a Hopf bifuration," Proceedings of the 31st IEEE Conference on Decision and Control, Dec. 16–18, 1992, Tucson, Arizona, IEEE Control Systems Society, 2113–2118.

Dynkin, E.B., 1965, "Markov Process I," Springer-Verlag, Berlin.

Frey, M., Simiu, E., 1993, "Noise-induced chaos and phase space flux," Physica D, Vol 63, 312–340.

Falzarano, J.M.,Shaw, S.W., Troesch, A.W., 1992, "Application of global methods for analyzing dynamical systems to ship roll motion and capsizing," Int. J. Bifurcation Chaos, Vol 2, 101–116.

Häckl, G., 1993, "Numerical approximation of reachable sets and control sets," Random and Computational Dynamics, Vol 1, 371–394.

Häckl, G., Schneider, R., 1994, "Controllability near a Takens-Bogdanov-Bifurcation." Preprint no. 115, Weierstraß-Institut für Angewandte Analysis und Stochastik.

Hsieh, S.-R.,Troesch, A.W., Shaw, S.W., 1994, "A nonlinear probabilistic method for predicting vessel capsizing in random beam seas," Proc. R. Soc. Lond., Vol A 446, 195–211.

Ikeda, N., Watanabe, S., 1981, "Stochastic Differential Equations and Diffusion Processes," North Holland.

Kliemann, W., 1987, "Recurrence and invariant measures for degenerate diffusions," Ann. Prob., Vol 15, 690–707.

Kliemann, W., 1988, "Analysis of nonlinear stochastic systems" in : Analysis and Estimation of Stochastic Mechanical Systems, W. Schiehlen and W. Wedig (eds.), Springer- Verlag, 43–102.

Kloeden, P., Platen, E., 1992, "Numerical Solution of Stochastic Differential Equations," Springer-Verlag, New York.

Kunita, H., 1974, "Diffusion Processes and Control Systems," Lecture Notes, University of Paris.

Mann, N.R., Schafer, R.E., Singpurwalla, N.D., 1974, "Methods for Statistical Analytical of Reliability and Life Data," John Wiley, New York.

Stroock, D.W., Varadhan, S.R.S., 1972, "On the support of diffusion processes with applications to the strong maximum principle," Proc. 6th Berkeley Symp. Math. Stat. Probab., Vol 3, 333–359.

Thompson, J.M.T., Rainey, R.C.T., Soliman, M.S., 1993, "Mechanics of ship capsize under direct and parametric wave excitation," Phil. Trans. R. Soc. Lond., Vol A 338, 471–490.